How to cite: *Angew. Chem. Int. Ed.* **2022,** *61,* e202201103
International Edition: doi.org/10.1002/anie.202201103
German Edition: doi.org/10.1002/ange.202201103

Metals in Medicine

Alkylgold(III) Complexes Undergo Unprecedented Photo-Induced β-Hydride Elimination and Reduction for Targeted Cancer Therapy

*Jia Jiang[+], Bei Cao[+], Yuting Chen[+], Hejiang Luo, Jiaying Xue, Xiaolin Xiong, and Taotao Zou**

Abstract: Spatiotemporally controllable activation of prodrugs within tumors is highly desirable for cancer therapy to minimize toxic side effects. Herein we report that stable alkylgold(III) complexes can undergo unprecedented photo-induced β-hydride elimination, releasing alkyl ligands and forming gold(III)-hydride intermediates that could be quickly converted into bioactive [Au^{III}–S] adducts; meanwhile, the remaining alkylgold(III) complexes can photo-catalytically reduce [Au^{III}–S] into more bioactive Au^{I} species. Such photoreactivities make it possible to functionalize gold complexes on the auxiliary alkyl ligands without attenuating the metal–biomacromolecule interactions. As a result, the gold(III) complexes containing glucose-functionalized alkyl ligands displayed efficient and tumor-selective uptake; notably, after one- or two-photon activation, the complexes exhibited high thioredoxin reductase (TrxR) inhibition, potent cytotoxicity, and strong antiangiogenesis and antitumor activities in vivo.

Introduction

There has been a burgeoning interest in developing prodrugs that can be controllably activated within tumors because they can minimize the toxic side effects on normal cells.[1] In past years, tremendous efforts have been made in developing stimuli-activatable prodrugs by using intrinsic tumor microenvironments or by external stimuli.[2] Among these endeavors, metal-based photoactivatable prodrugs, or photoactivated chemotherapies (PACTs) are highly attractive for their spatiotemporal resolution during cancer treatment.[3] For example, Pt^{IV} complexes can be photochemically or photo-catalytically reduced into active Pt^{II} species for DNA binding;[4] Ru^{II} complexes can efficiently undergo photo-induced ligand dissociation to release bioactive ligands and/or to allow for DNA binding via metal coordination.[5] Of particular interest are those prodrugs in which tumor-targeting moieties are introduced as auxiliary ligands to improve the tumor specificity without attenuating the bioactivity of the parent compounds.[4e,6] Nonetheless, despite being highly promising,[7] only a handful of PACT complexes are available in the literature and their photoreactivities are largely restricted to photo-reduction or -substitution reactions by breaking not-so-strong bonds such as Pt–O/N and Ru–N/S.[3d] It is challenging to develop photo-reactions based on activating robust bonds such as M–C bond (M = Pt, Au, Ru, Rh…, C = carbanion ligands) in noble metal organometallic complexes[8] that can fully resist strong nucleophiles and reductants for the avoidance of systemic adverse effects.

Gold complexes have well-known anti-proliferative activity towards various cancer cells including the cisplatin-resistant variants.[9] Such activities are due to their high binding affinity towards thiol- and/or selenol-enzyme targets such as thioredoxin reductase (TrxR) that is overexpressed in many tumors.[10] However, the high redox potential (Au^{3+}/Au^{+} 1.36 V, Au^{+}/Au^{0} 1.83 V)[11] and the strong thiol-affinity of gold posed big hurdles to develop gold complexes with enough stability to combat off-target interactions and with high tumor-specificity to minimize side effects.[2g] Pioneering works of using strong donor ligands such as phosphine,[12] N-heterocyclic carbene (NHC),[13] alkyne,[12b,14] dithiocarbamate,[15] porphyrin,[16] and cyclometalated ligand[17] have shown the ability to improve the anti-tumor activity of gold complexes. In efforts to develop photo-activatable prodrugs, we have previously reported that cyclometalated gold(III) complexes containing hydride ligand [(C^N^C)AuH] (H_2C^N^C = 2,6-diphenylpyridine, **1a**, Figure 1) can undergo photo-induced hydride-substitution to activate its thiol-reactivity and anti-cancer activity;[7g] however, the hydride ligand cannot be modified to tune the physiochemical properties such as water solubility and tumor-specificity that are critical for further drug development.

In the literature, certain d^8 metal complexes (e.g., Ni^{II}-phthalocyanine, Pt^{II}-terpyridines) were known to induce axial ligation at the excited state via the expanded coordination sites.[18] In view that the electrophilic metal complexes with open coordination sites could proceed with β-hydride elimination,[19] it is conceived that the isoelectronic d^8 Au^{III} complexes containing alkyl ligands may undergo photo-

[*] J. Jiang,[+] Y. Chen,[+] H. Luo, J. Xue, Dr. X. Xiong, Prof. Dr. T. Zou
Guangdong Key Laboratory of Chiral Molecule and Drug Discovery
School of Pharmaceutical Sciences
Sun Yat-Sen University
Guangzhou 510006 (P. R. China)
E-mail: zoutt3@mail.sysu.edu.cn
Dr. B. Cao[+]
Warshel Institute for Computational Biology
and General Education Division
The Chinese University of Hong Kong
Shenzhen 518172 (P. R. China)
[+] These authors contributed equally to this work

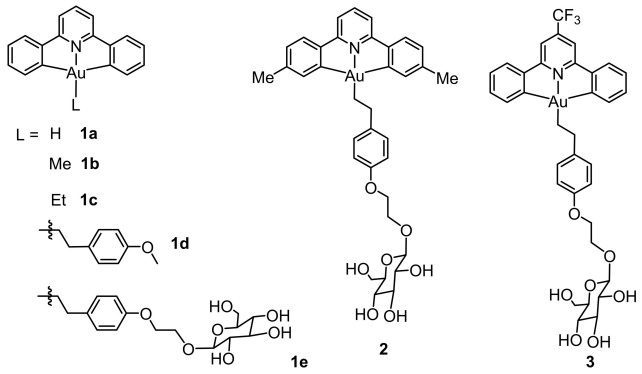

Figure 1. Chemical structure of gold(III) complexes.

induced β-H elimination to form the gold(III)-hydride species,[20,21] which could be harnessed to develop next-generation gold-based prodrugs. Herein we report a type of stable alkylgold(III) complexes that can efficiently initiate photo-induced β-H elimination followed by photocatalytic reduction to controllably release active gold species, rendering the complexes to display efficient cellular uptake, potent inhibition on thioredoxin reductase (TrxR), strong and cancer-selective cytotoxicity in vitro, and antiangiogenic and anti-tumor activities in vivo. To the best of our knowledge, it is the first time that the photo-induced β-hydride elimination reaction is identified for robust prodrug activation.

Results and Discussion

Synthesis, Solution Stability and Photochemistry

The cyclometalated gold(III)-alkyl complexes **1b** and **1c** (Figure 1) were synthesized by reacting [(C^N^C)AuOAc^F] with Grignard reagents,[21] and **1d**, **1e**, **2**, and **3** were prepared from the reaction of [(C^N^C)AuH] with styrene derivatives in the presence of radical initiator azodiisobutyronitrile (AIBN). These complexes are highly soluble (> 10 mM) in THF, CH_2Cl_2, DMF and DMSO, and they have been fully characterized by ^{1}H NMR, ^{13}C NMR, high-resolution mass spectrometry (HRMS), HPLC and elemental analysis (Supporting Information, Figure S1–S6). The ^{1}H-^{1}H COSY/NOESY NMR of **1c** and **1e** have also been performed (Figure S7). Unless otherwise mentioned, the gold(III) complexes were dissolved in DMSO to prepare a 10 mM stock solution and then diluted in aqueous solution for the following experiments.

The stability of the alkylgold(III) complexes was firstly examined. Taking **1c** as an example, after 48 h incubation in dark, it did not show noticeable change in the UV/Vis absorption spectra or in the LC chromatograms in DMSO, DMSO/H_2O (1/1, v/v) or DMSO/PBS (1/1, v/v) with or without 100 equiv of N-acetylcysteine (NAC) or sodium ascorbate (Figure S8a–e), indicative of high thiol stability. However, UV/Vis experiments revealed that upon 365 nm light irradiation in DMSO, **1c** displayed red shift of vibronic absorption and increase of absorbance at 350–410 nm which became levelled-off in 20 min (Figure 2b). The reaction quantum yield ϕ[22] was calculated to be 0.028 (Figure S9) that is comparable to the photo-reactivity of **1a** ($\phi = 0.018$, Figure S9). Interestingly, in the presence of 10 equiv (1 mM) of NAC, the vibronic absorption at 350–410 nm gradually vanished (Figure 2c) after 365 nm light irradiation, and in 10 mM of NAC, the vibronic absorption decreased even faster (Figure 2d).

The photo-reactions were then studied by HPLC (Figure 2e). In the absence of NAC, **1c** (retention time 15.68 min) gradually disappeared in association with a new peak at 12.14 min (Figure 2e and S10), which was identified to be [Au(C^N^C)(DMSO)] (Figure S10). Notably, this peak could be similarly generated from [Au(C^N^C)H] (**1a**) in DMSO under light irradiation (Figure S11). By using ^{1}H NMR, a singlet peak at 5.43 ppm was detected after irradiating **1c** in d_6-DMSO for 30 min (Figure 2f), and this peak disappeared after bubbling with N_2, indicative of forming C_2H_4;[23] for **1d** after light irradiation, 4-methoxystyrene and [Au(C^N^C)-(DMSO)] were detected in the LC chromatogram as well (Figure S12). When performing the ^{1}H NMR experiment in $CDCl_3$ for **1c** (Figure S13), besides C_2H_4 (5.40 ppm), $CHDCl_2$ with a signature 1:1:1 triplet at 5.28 ppm ($J = 1.1$ Hz) was detected, suggesting formation of a short-lived metal-hydride species.[24] Thus, photo-induced β-hydride elimination reaction likely occurred which simultaneously generated alkene and hydride intermediate that further underwent a hydride transfer reaction. For comparison, **1b** containing the methanide ligand slowly decomposed by ≈30 % in DMSO after 20 min light irradiation by forming uncharacterizable peaks in the LC chromatogram (Figure S14).

In the presence of 1 mM of NAC and under light irradiation (Figure 2e and S15a), **1c** disappeared slightly faster in the LC chromatogram accompanied by generating a dominant peak of [Au(C^N^C)-NAC] adduct at 7.16 min (Figure S15a), and this product could be similarly generated by reacting **1a** with NAC (Figure S15b). In the meantime, a minor peak at 7.03 min appeared after 5 min of photo irradiation showing m/z of 393.2 (M+1, Figure S16) that could be attributed to C^N^C-NAC losing the Au ion, and this peak became more notable with elongated photo-irradiation (Figure S15a); meanwhile, in the negative mode of mass spectra, a peak with m/z of 521.2 consistent with forming $[Au(NAC)_2]^-$ was found (Figure S17). When 10 mM of NAC was present (a reachable cellular thiol concentration),[25] the peak at 7.16 min was initially formed in association with a minor but more remarkable one at 7.03 min after 5 min light irradiation (Figure 2e); interestingly, the peak intensity at 7.16 min gradually decreased while that at 7.03 min became more dominant upon further photo-irradiation, with intensity ratio at 7.03 min vs 7.16 min from 3:7 after 5 min irradiation, to 6:4 after 10 min, and 8:2 after 15 min (Figure 2e), implying [Au(C^N^C)NAC] to C^N^C-NAC conversion. Therefore, two reaction processes happened for **1c** with NAC: firstly, **1c** initiated photo-induced β-hydride elimination by generating ethylene and [Au(C^N^C)H] with the latter product being quickly

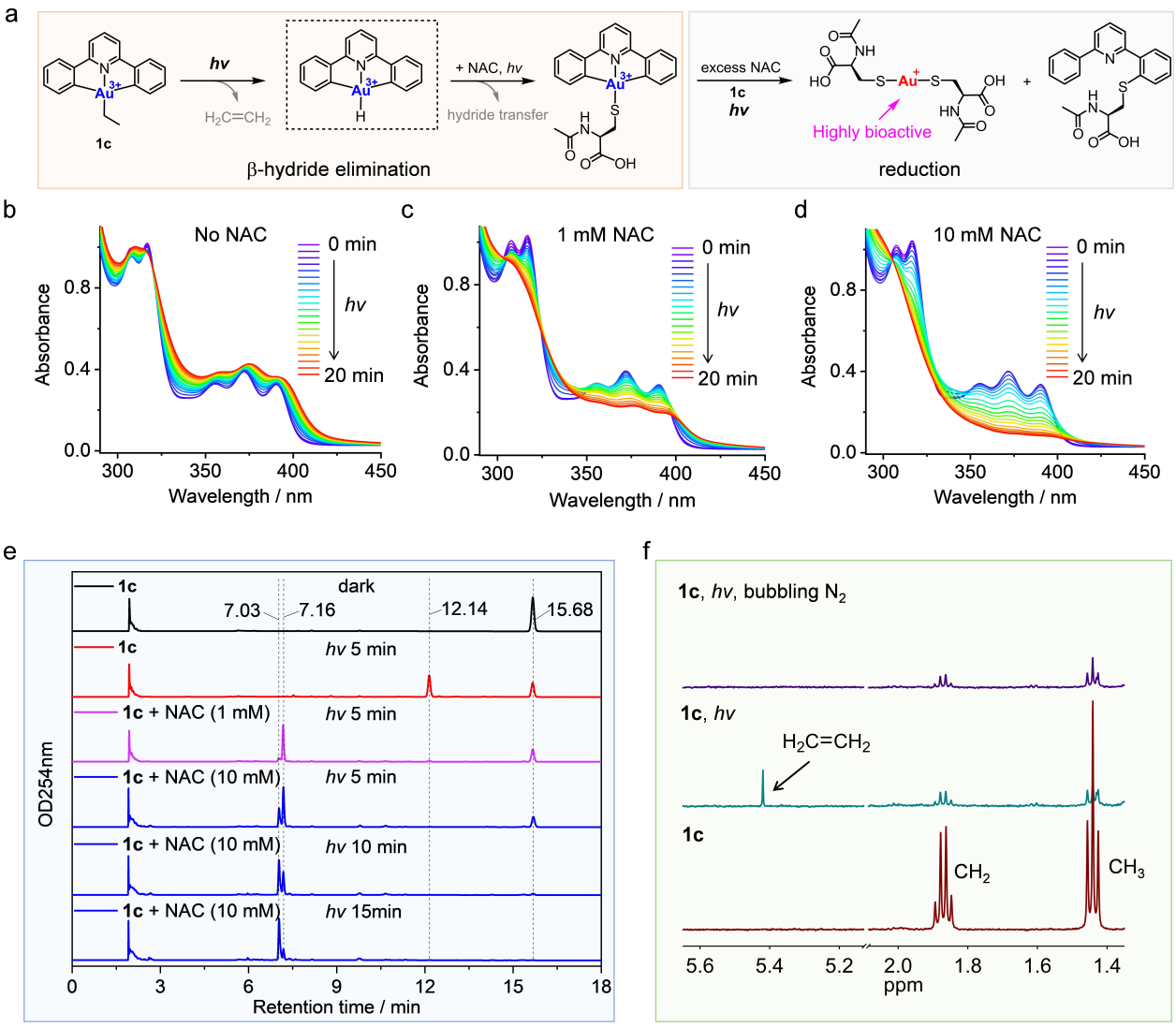

Figure 2. The photo-reactivity of **1c**. a) Reaction of **1c** with NAC under light irradiation. b–d) UV-vis absorption spectra of **1c** (100 μM) in the absence (b) or presence of 1 mM (c) or 10 mM (d) of NAC under 365 nm light irradiation in 20 min. e) LC chromatograms for the reaction of **1c** with or without 1 or 10 mM of NAC after 365 nm light irradiation for 5, 10 or 15 min in DMSO. f) ^{1}H NMR for the photo-reaction of **1c** in d_6-DMSO after 365 nm irradiation for 30 min, showing ethylene formation.

converted into [Au(C^N^C)NAC]; then, [Au(C^N^C)NAC] was reduced into C^N^C-NAC and [Au(NAC)$_2$]$^-$ (Figure 2a). In contrast, **1b** reacted with NAC in a slower rate by forming several new peaks in the LC chromatogram and no [Au(C^N^C)NAC] was detected (Figure S18).

Mechanism Study

To elaborate the photo-induced β-hydride elimination reaction, additional experiments were performed. We found the reverse reaction can happen as well. When mixing [Au(C^N^C)H] with 4-methoxystyrene in a non-coordinative solvent such as EtOAc, **1d** was obtained in 15–18 % yield after 365 nm light irradiation for 10 min (by HPLC and ^{1}H NMR, Figure 3a, and S19), suggestive of the microscopic reversibility of the reaction that is characteristic of β-hydride elimination.[19c,20b] Then, computational calculations were performed to understand the mechanism based on DFT and TDDFT using generalized gradient approximation exchange-correlation density functional PW91 and basis set of 6-31G* except Stuttgart/Dresden ECP(SDD) for Au. As depicted in Figure 3b, S20 and Table S1, S2, the natural transition orbital analyses of the triplet (T_1) excited state show that the electron is mainly localized in pyridine (57 %) and the two phenyl moieties (30 %), whereas the hole is located at the phenyl rings (72 %) together with a significant portion at Au (24 %). Thus the gold(III) complex has a triplet phenyl-to-pyridine intra-ligand (^{3}IL) charge transfer mixed with triplet metal-to-ligand charge transfer (^{3}MLCT) character,[21] rendering the Au ion to be highly electrophilic that may favor the axial coordination.[18a] In the meantime, while **1c** displays an ideal square planar geometry at S_0, it

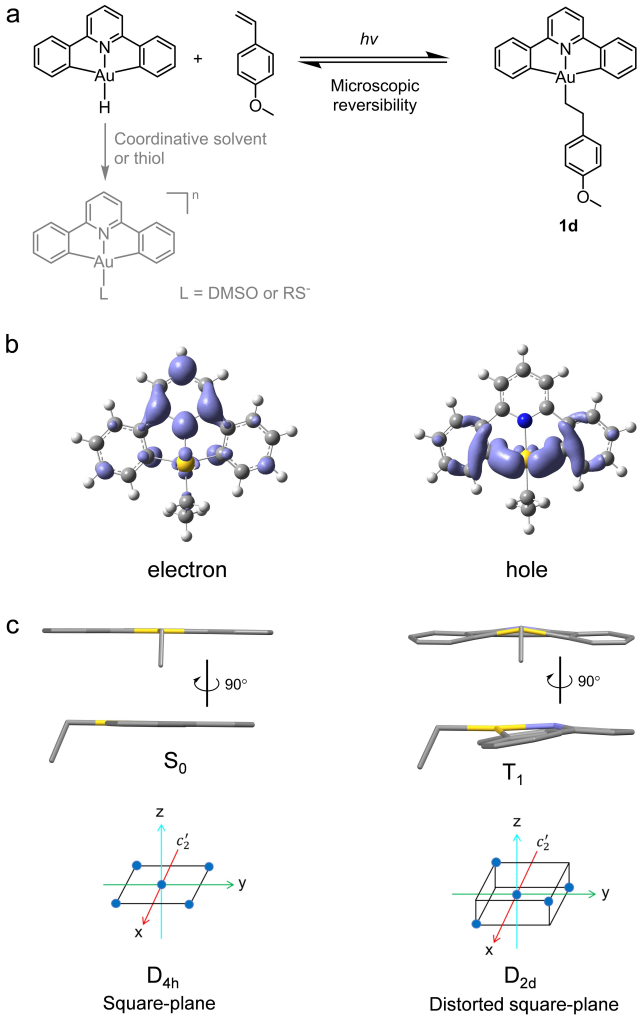

Figure 3. Mechanism studies. a) Photoreaction of **1a** with 4-methoxystyrene in non-coordinative solvents, which is reverse to the photo-induced β-H elimination. b) Electron–hole distribution of **1c** at T_1 excited state. c) The optimized geometry of **1c** at S_0 and T_1 states. The symmetry groups of D_{4h} and D_{2d} are also shown.[28]

becomes distorted showing out-of-plane bending of the cyclometalated ligand at the T_1 excited state (Figure 3c), which is typical of symmetry decrease from pseudo D_{4h} to D_{2d} for d^8 complexes at the excited states,[26] leading to metal-centred (MC) ^{3}d–d excited states lying close to the ^{3}MLCT and ^{3}LC excited states (Figure S21).[27] Indeed, the molecular orbital analyses show that the T_1 excited state of **1c** involves a minor but noticeable $d_{x^2-y^2}$ orbital in its electron composition (Figure S20), which is consistent with the engagement of low lying ^{3}d–d state. In the literature, the ^{3}d-d excited state has been known to expand the coordination number and favor axial coordination as in the case of Ni^{II}-porphyrins.[18b] Therefore, the photo-induced electrophilic character and the possible involvement of ^{3}d–d excited states make it possible for **1c** to take the vacant site for the β-hydride elimination to occur.

Afterwards, we tried to understand the mechanism for $[Au(NAC)_2]^-$ formation. As shown in Figure 2e, C^N^C-NAC was generated from [Au(C^N^C)NAC]. However, when [Au(C^N^C)NAC] was directly irradiated with light, no reactions occurred in the absence or presence of NAC or 4-methoxystyrene (Figure S22a–c). On the other hand, it was noticed that during the transformation, the reaction mixture always contained a tiny but observable amount of **1c** in the LC chromatogram (Figure 2e and S15), which may additionally act as a photocatalyst. To verify this hypothesis, the analogue complex $[Au(C^N^C)(NHC)]^+$ or **1b** (0.5 or 1 equiv) was added in the mixture of [Au(C^N^C)NAC] (100 μM) and NAC (10 mM), complete conversion of [Au-(C^N^C)NAC] into C^N^C-NAC was found within 10 min of light irradiation (Figure S23 and S24), implying that the photo-catalysts are indeed active for photoreduction. In fact, we found that the reduced form of **1c**, which could be generated from the reductive quenching of its excited state by thiols (Figure S25), is a strong reductant ($[Au^{III}]/[Au^{II}] = -1.92$ V, Figure S26) that can convert [Au(C^N^C)NAC] (reduction potential of −1.02 V, Figure S26b) into C^N^C-NAC and $[Au(NAC)_2]^-$. Therefore, besides photo-induced β-H elimination, **1c** additionally acted as a photocatalyst to reduce the $[Au^{III}–S]$ adduct into C^N^C-NAC and $[Au-(NAC)_2]^-$.

Photo-Activated In Vitro Activities

Complex **1d**, with 4-methoxystyrene derivative as auxiliary ligand, proceeded with the dual photo-induced β-H elimination and photo-reduction as efficiently as **1c** (Figure S27). Thus, it became feasible to introduce functional groups into the gold complexes by styrene derivatives. Complexes **1e**, **2**, and **3** containing glucose moieties were synthesized to tune the water solubility and tumor-targeting capability. Of note, by bringing in either methyl group on the phenyl ring (**2**) or $–CF_3$ moiety on the pyridine ring (**3**) of C^N^C ligand, the gold complexes were endowed with absorption at visible region (Figure S28). Like **1c**, complexes **1e**, **2**, and **3** showed good thiol-stability and displayed comparable or even higher photo-reactivity based on UV/Vis analysis (Figure S29) or HPLC experiments (Figure S30).

Subsequently, the cellular stability and photo-reactivities of the gold(III) complexes were tested. Human melanoma A375 cells were incubated with 100 μM of **3** for 12–36 h, and then the cells were washed and lysed, followed by acetone precipitation. After analysing the supernatant by HPLC (Figure S31), a significant amount of **3** (retention time 12.35 min) was detected, and this peak gradually decreased with elongated incubation accompanied by forming a new species with retention time at 15.23 min that was identified to be the glucose-hydrolyzed product [Au(C^N^C)-$(CH_2)_2$-Ph-*p*OCH_2CH_2OH] (**13**) in which the cyclometalated gold-(III)-alkyl scaffold remained intact. Similar activities were found in A549 lung cancer cells and for **1e** and **2** (Figure S32 and S33). However, when **3**-treated A375 cells were irradiated with light before cell lysing, neither the complex nor the glucose-hydrolysed product were detected in the supernatant by HPLC (data not shown). Instead, inductively coupled plasma-mass spectrometry (ICP-MS) analysis of the

insoluble proteins after acetone precipitation showed the amount of protein-bound gold (13.3 ng per 10^5 cells) is 2.2-fold higher than that in the dark condition (5.9 ng per 10^5 cells), suggesting the activation of thiol-reactivity of the gold complexes.

Next, we investigated whether the photo-activated gold complexes can inhibit TrxR. A375 cells were treated by the gold complexes for 2 h, followed by light irradiation and a further 2 h incubation, and then the TrxR activity was measured (Table 1, Figure S34). Results showed that **1c** inhibited TrxR with IC_{50} of 8.04 μM that was slightly weaker than **1a** ($IC_{50}=3.18$ μM) but more potent than **1b** ($IC_{50}=11.1$ μM). Notably, complex **3** displayed extremely strong inhibition on TrxR with IC_{50} of 0.79 μM that was comparable to auranofin ($IC_{50}=0.68$ μM). Consistent with the stability test, in dark condition, all the gold(III) complexes did not show inhibitory activity ($IC_{50}>100$ μM, Table 1).

To understand the mechanism of TrxR inhibition, we examined the binding preference of the photoactivated gold(III) complex towards nucleophilic amino acids including Glu, His, Met, Cys and Sec by HRMS. After incubating the equimolar ratio mixture of **1e**/Glu/His/Met/Cys under 365 nm light irradiation for 20 min, peaks with *m/z* of 545.0618 and 436.9914 were found, indicative of forming [Au(C^N^C)-Cys] and $[Au(Cys)_2]^-$ (Figure S35a), but no adducts with Glu, His or Met were found. If 1 equiv of Sec is additionally added in the reaction mixture (**1e**/Glu/His/Met/Cys/Sec), the adducts with isotopic pattern and *m/z* (Figure S35b) consistent with [Au(C^N^C)-Cys] and $[Au(Sec)_2]^-$ were detected, without noticeable adduct with other amino acids, suggesting the binding preference towards Sec and Cys.[10b,29] Importantly, when Sec- and Cys-containing TrxR C-terminal GCUG tetrapeptide was mixed with equimolar of **1e** and irradiated with 365 nm light for 20 min, the product agreeing with a single Au^+ ion simultaneously binding to S and Se of GCUG ([GCUG-Au-2H] $m/z=580.9674$, Figure S35c) was found. In the model proteins of BSA and HSA containing free Cys, adducts formation were observed, giving *m/z* of 66861.40 (vs intact BSA *m/z* 66436.40, Figure S36) and 66875.70 (vs intact HSA *m/z* 66450.70, Figure S37), respectively, attributed to the attachment of [Au(C^N^C)] moiety to the proteins, thus supporting the possible involvement of direct binding of photoactivated gold with the Sec/Cys motif for TrxR inhibition.[30]

In light of the photo-activated TrxR inhibition on cancer cells, the cytotoxicity of the photo-activatable gold complexes (**1c–e**, **2**, and **3**) was examined in different human cancer cells including colorectal carcinoma HCT116, melanoma A375, hepatocellular carcinoma HepG2, non-small cell lung carcinoma A549, breast cancer MCF-7, and triple-negative breast cancer MDA-MB-231. In general, cancer cells were treated with the gold(III) complex for 2 h, followed by 5 or 10 min light irradiation; after a total 24 h incubation, the cytotoxicity was evaluated by MTT assay. It turned out that while the gold(III) complexes did not show obvious cytotoxicity in the dark with $IC_{50}>100$ μM (except **1e** with $IC_{50}>20$ μM), they were highly cytotoxic with IC_{50} of 0.25–23.3 μM in light (Table S3). Of significance was the cytotoxicity of the glucose-containing **1e**, **2**, and **3** showing sub-micromolar IC_{50} values and up to 400-fold photo-index ($IC_{50,dark}/IC_{50,light}$) that was much stronger than **1c** and **1d**. For comparison, cisplatin and auranofin did not show obvious change of IC_{50} after light irradiation (Table S3). In addition, we tested whether the photoactivated gold complex at extracellular medium contributed to the photocytotoxicity or not by replacing the drug-containing medium after 2 h incubation with fresh one (Figure S38). Results showed that the photocytotoxicity of the gold(III) complex (**1e** as an example) did not change (IC_{50} of 0.29 ± 0.01 μM) compared to the condition without changing medium (IC_{50} of 0.32 ± 0.03 μM), indicating that the photocytotoxicity was mainly caused by the intracellularly photoactivated gold(III) complexes.

We also studied whether the photocytotoxicity involved direct generation of reactive oxygen species by co-treatment of **3** with $^1O_2$ suppresser NaN_3 (5 mM), or $OH^\bullet$ inhibitor d-mannitol (50 mM), or $O_2^{\bullet-}$ scavenger tiron (5 mM). The photocytotoxicity IC_{50} was found to be 0.86 μM, 0.73 μM, 0.98 μM, respectively, which was similar to its original photocytotoxicity IC_{50} of 0.74 μM, indictive of little to low contribution of direct photo-induced ROS (Table S4). For comparison, the photocytotoxicity of the less reactive **1b** was more significantly influenced by these ROS inhibitors (Table S4).

For the glucose-containing complexes such as **3**, the cyclometalated gold(III)-alkyl scaffold is planar and hydrophobic, whereas the glucose moiety is hydrophilic (Figure 4a); such an amphiphilic character may render the complex with a self-assembly property.[31] Indeed, dynamic light scattering (DLS) study showed that **3** formed nanoparticles with an average size of 160 nm in aqueous solution (Figure 4b), and transmission electron microscopy (TEM) analysis also revealed that **3** formed pseudo round-shaped nanoparticles with a slightly smaller size of ≈90 nm (Figure 4c). Then we examined whether the self-assembly property contributed to the mechanism of uptake. HCT116, HepG2 or A375 cells were co-treated with **3** and dynamin-dependent endocytosis inhibitor dynasore (DNS, Figure 4d and S39a) or clathrin-mediated endocytosis blocker chlorpromazine (CPZ, Figure 4e, S39b), both at a non-toxic 10 μM concentration. MTT assay showed that the photocytotoxicity of **3** was significantly decreased by DNS with IC_{50} value raising from 5.0 μM to 10.3 μM ($p<0.01$) and diminished by CPZ with IC_{50} from 2.1 μM to 5.8 μM ($p<0.0001$). In the meantime, the glucose transporter (GLUT) inhibitor phlorizin (Pz) also attenuated the photocytotoxicity of **3** from $IC_{50}=1.4$ μM to $IC_{50}=2.1$ μM ($p<0.001$, Fig-

Table 1: TrxR inhibition activity (IC_{50}, μM) of A375 cells after treatment by the gold complexes. The cells were treated with each complex for 2 h and were then irradiated with light, followed by a further 2 h incubation. The TrxR activity of the cell lysates was measured.

Entry	**1a**[a]	**1b**[a]	**1c**[a]	**3**[b]	Auranofin
Dark	>100	>100	>100	>100	0.68±0.21
Light	3.18±0.52	11.1±0.1	8.04±0.90	0.79±0.02	–

[a] 365 nm irradiation for 5 min. [b] 420 nm irradiation for 10 min.

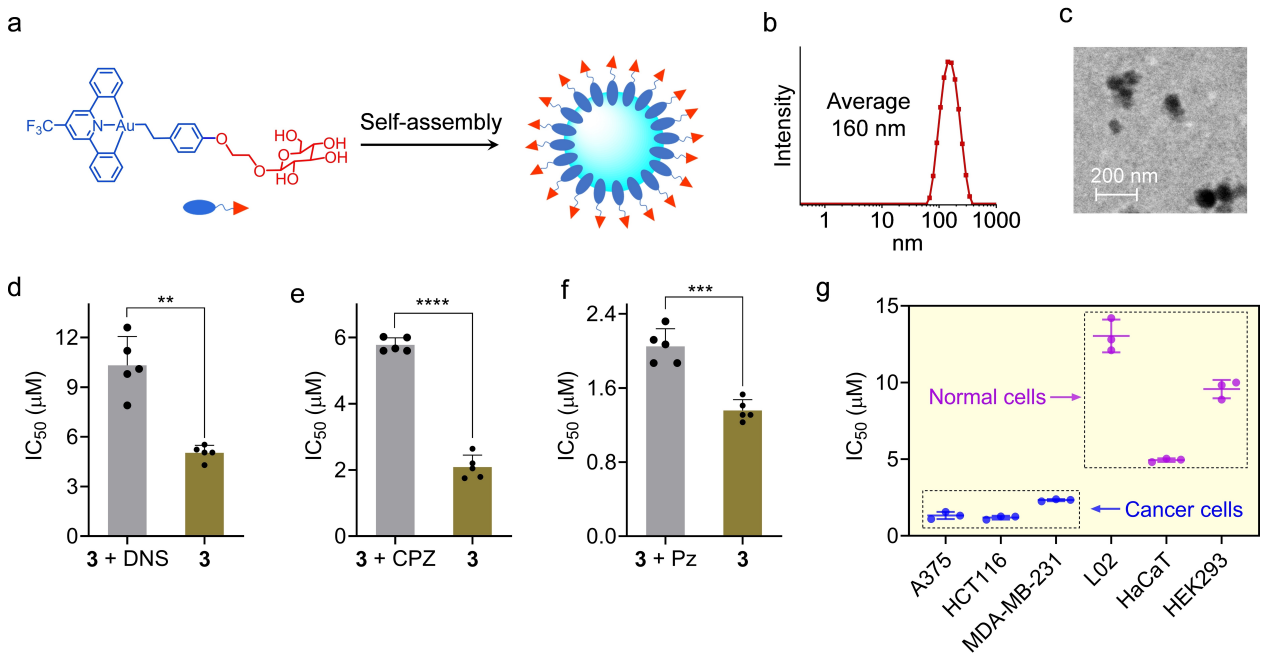

Figure 4. Tumor-selectivity of complex **3**. a) Self-assembly of **3** in aqueous solution to form nanoparticles. b, c) DLS (b) and TEM (c) analysis of the aqueous solution of **3** at 50 μM. d–f) Influence of photo-cytotoxicity of **3** on HCT116 cells after co-treatment by dynamin-dependent endocytosis inhibitor dynasore (DNS, 10 μM, in no FBS condition, d), clathrin-mediated endocytosis blocker chlorpromazine (CPZ, 10 μM, e), and glucose transporter inhibitor phlorizin (Pz, 2 mM, f). g) Photocytotoxicity of **3** towards different types of cancer and normal cells.

ure 4f). The reduced cytotoxicity after co-treatment of **3** with DNS, CPZ and Pz is consistent with the attenuated cellular uptake as revealed from ICP-MS analysis (Figure S40) showing 79.7 %, 64.7 % and 51.2 % of gold content, respectively, compared to the treatment by **3** only. These results collectively indicate a GLUT-associated endocytosis cellular uptake mechanism.

In the literature, many cancer cells have been reported to abnormally overexpress GLUT.[32] Accordingly, the photocytotoxicity of **3** towards normal cells was explored for comparative study (Figure 4g). Encouragingly, results showed that the gold complex was generally less cytotoxic towards normal cells including human hepatic cell line L02 (IC_{50} = 12.8 μM), epidermal keratinocyte line HaCaT (IC_{50} = 5.0 μM), and embryonic kidney 293 cell line HEK293 (IC_{50} = 9.8 μM) than that towards cancer cells such as A375, HCT116, and MDA-MB-231, with IC_{50} of 1.25–2.40 μM, i.e., up to 10-fold selectivity. Compared to **3**, complex **1c** displayed 3.8- to 5.7-fold lower cytotoxicity towards these cancer cells but 1.9- to 3.1-fold higher cytotoxicity to the normal cells under similar conditions (Table S5).

Photo-Activated In Vivo Activities

The in vivo anti-tumor activities of the gold(III) complexes were then examined. As reported before, reactive gold(I) is highly effective in inhibiting tumor-associated angiogenesis.[12b] Herein the embryo of transgenic zebrafish (GFP-flk) was treated with **3** for 12 h and then irradiated with 420 nm light for 30 min. After 3 days of embryonic development, the group treated by **3** with light irradiation showed significantly impaired vasculature particularly in the dorsal longitudinal anastomotic vessel (DLAV) as depicted in Figure 5a. In contrast, for the **3**-treated group in dark or the light-only control group, there was no such damage (Figure 5a).

We further performed the anti-tumor activity of the gold(III) complexes in mouse models. After treatment of mice bearing A375 xenograft with 3 mg kg^{-1} of **3** (i.p.) followed by 420 nm light irradiation for 10 min once every two or three days, significant inhibition of tumor volume by 85 % (versus solvent group, $p < 0.05$) was observed after treating for 18 days (Figure 5b). The treatment did not cause mouse death or body weight loss (Figure 5b). In the control experiments, **3** in the dark or light irradiation only did not show obvious inhibition (Figure 5b).

Two-Photon Activation

Since certain cyclometalated metal complexes could be excited by two-photons,[1e,7g] we tested the possibility of long-wavelength laser irradiation to activate the gold(III)-alkyl complexes. A375 cells were treated with **3** for 2 h followed by laser irradiation at 800 nm (0.52 W) for 5 min. The living/dead cells were analyzed by co-treatment with ethidium homodimer-1 that can specifically stain dead cells (red emission) and Calcein AM that can distinguish living cells (green fluorescence). As depicted in Figure S41, red emission was only found in the laser-irradiated area of **3**-treated cells where no green emission was detected; in

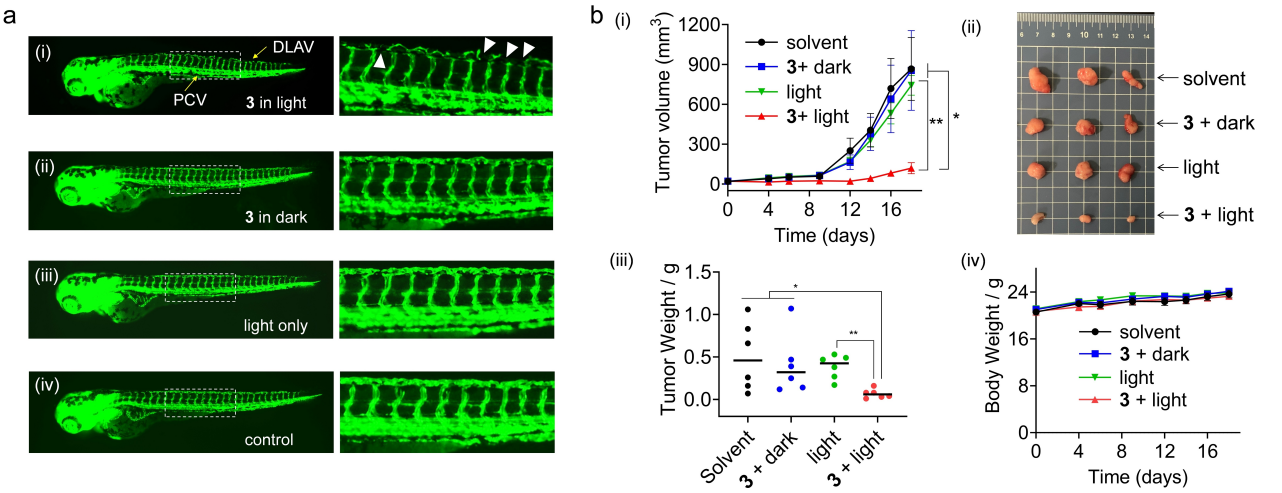

Figure 5. Antiangiogenic and antitumor activities in vivo. a) Inhibition of blood vessel formation during zebrafish embryo development after treatment by **3** (125 μM) under 420 nm light irradiation for 30 min (i) or in dark (ii) or by light only (iii) or by no treatment (iv). b) Change of tumor volume (i) and body weight (ii) after treatment of mice bearing A375 xenografts by **3** under 420 nm light irradiation 10 min per day, or by **3** in the dark, or by solvent control, or only by light irradiation. The representative images of tumors after sacrifice of mice on day 18 were shown.

contrast, only green fluorescence but not red emission was found in the surrounding non-irradiated region. In the control group with laser irradiation only, there was no red emission. Thus, the gold(III) complex is indeed activatable by two-photon irradiation that may benefit tumor treatment needing a deeper penetration.

Conclusion

In conclusion, alkylgold(III) complexes are found to proceed with unprecedented dual photo-reactivities to controllably release bioactive gold species with high tumor specificity. They are stable against thiols and ascorbates in the dark but become highly reactive to initiate β-hydride eliminations, which release the alkyl ligand and form [Au(C^N^C)H] that can be further transformed into the [Au^{III}–S] adduct. Such a reactivity makes it possible to functionalize the gold(III) complexes at the auxiliary alkyl moieties without diminishing the binding interactions towards enzyme target(s). In this regard, a glucose moiety is introduced, leading to efficient and tumor-selective cellular uptake. In the meantime, the [Au^{III}–S] adduct could be further photo-catalytically reduced into more active Au^{I} species, a phenomenon that is similar to the photocatalytic reduction of Pt^{IV} prodrugs[4d,33] but has not been reported for gold complexes. Consequently, after one- or two-photon irradiation, the gold complex was found to strongly inhibit cellular TrxR, display up to >400-fold increases of cytotoxicity, and strong antiangiogenic and anti-tumor activities in animal models. These results collectively demonstrate that our strategy by harnessing the dual photo-reactivities of alkylgold(III) complexes can not only spatiotemporally control the reactivity of gold against off-target interactions but also enable to effectively tune the drug-like properties such as solubility and formulation for in vivo tumor-targeted therapies.

For PACT complexes in the literature, the M–O, M–N or M–S bonds were usually constructed which were responsible for photo-substitution or -reduction reactions. While these metal–ligand bonds have proven stable in certain metal prodrugs, these donor ligands may not construct stable complexes for metals with high redox potential or with high binding affinity to physiological nucleophiles as in the case of gold-based drugs. In this work, we uncovered a strategy for photoactivated prodrugs based on breaking the strong M–C bond into a reactive M–H bond by photo-induced β-hydride elimination. The alkylgold(III) complexes are highly stable and can meanwhile efficiently undergo such an elimination reaction and the following reduction to spatiotemporally deliver active gold species within tumor tissues. Since β-hydride elimination is a common organometallic reaction and many metal complexes are known to be electrophilic at excited states where vacant or expanded coordination sites are possibly available for β-hydride elimination to happen, it is believed that the novel photoreactions of building gold-based prodrugs could be extended to other metal centers such as the isoelectronic Pt^{2+} to construct prodrugs with good stability, high tumor selectivity, and low side effects.

Experimental Section

All the characterization data, experimental procedures and supporting figures/tables are included in the Supporting Information.

Acknowledgements

This work was finically supported by National Natural Science Foundation of China (No. 22122706), Guangdong Science and Technology Department (No. 2019QN01C125), Guangdong Basic and Applied Basic Research Foundation

(No. 2021A1515012347, 2020A1515110508), Guangzhou Science and Technology Projects (No. 202102020790) and Guangdong Provincial Key Lab of Chiral Molecule and Drug Discovery (No. 2019B030301005). The Warshel Institute for Computational Biology funding from Shenzhen City and Long-gang District is also acknowledged.

Conflict of Interest

The authors declare no conflict of interest.

Data Availability Statement

The data that support the findings of this study are available from the corresponding author upon reasonable request.

Keywords: Anti-Cancer Metallodrug · Gold Medicine · Metal Prodrug · Photoactivated Chemotherapy · Thioredoxin Reductase

[1] a) S. Neidle, D. E. Thurston, *Nat. Rev. Cancer* **2005**, *5*, 285–296; b) T. C. Johnstone, K. Suntharalingam, S. J. Lippard, *Chem. Rev.* **2016**, *116*, 3436–3486; c) X. Wang, X. Wang, S. Jin, N. Muhammad, Z. Guo, *Chem. Rev.* **2019**, *119*, 1138–1192; d) E. J. Anthony, E. M. Bolitho, H. E. Bridgewater, O. W. L. Carter, J. M. Donnelly, C. Imberti, E. C. Lant, F. Lermyte, R. J. Needham, M. Palau, P. J. Sadler, H. Shi, F.-X. Wang, W.-Y. Zhang, Z. Zhang, *Chem. Sci.* **2020**, *11*, 12888–12917; e) E. Boros, P. J. Dyson, G. Gasser, *Chem* **2020**, *6*, 41–60.

[2] a) X. Wang, Z. Guo, *Chem. Soc. Rev.* **2013**, *42*, 202–224; b) M. Imran, W. Ayub, I. S. Butler, R. Zia ur, *Coord. Chem. Rev.* **2018**, *376*, 405–429; c) A. Sharma, M.-G. Lee, H. Shi, M. Won, J. F. Arambula, J. L. Sessler, J. Y. Lee, S.-G. Chi, J. S. Kim, *Chem* **2018**, *4*, 2370–2383; d) Z. Du, C. Liu, H. Song, P. Scott, Z. Liu, J. Ren, X. Qu, *Chem* **2020**, *6*, 2060–2072; e) Z. Xu, Z. Wang, Z. Deng, G. Zhu, *Coord. Chem. Rev.* **2021**, *442*, 213991; f) N. Nayeem, M. Contel, *Chem. Eur. J.* **2021**, *27*, 8891–8917; g) Y. Long, B. Cao, X. Xiong, A. S. C. Chan, R. W.-Y. Sun, T. Zou, *Angew. Chem. Int. Ed.* **2021**, *60*, 4133–4141; *Angew. Chem.* **2021**, *133*, 4179–4187; h) J. Geng, Y. Zhang, Q. Gao, K. Neumann, H. Dong, H. Porter, M. Potter, H. Ren, D. Argyle, M. Bradley, *Nat. Chem.* **2021**, *13*, 805–810.

[3] a) N. J. Farrer, L. Salassa, P. J. Sadler, *Dalton Trans.* **2009**, 10690–10701; b) T. A. Shell, D. S. Lawrence, *Acc. Chem. Res.* **2015**, *48*, 2866–2874; c) J. D. Knoll, C. Turro, *Coord. Chem. Rev.* **2015**, *282–283*, 110–126; d) S. Bonnet, *Dalton Trans.* **2018**, *47*, 10330–10343; e) C. Imberti, P. Zhang, H. Huang, P. J. Sadler, *Angew. Chem. Int. Ed.* **2020**, *59*, 61–73; *Angew. Chem.* **2020**, *132*, 61–73; f) M. Martínez-Alonso, G. Gasser, *Coord. Chem. Rev.* **2021**, *434*, 213736.

[4] a) J. S. Butler, J. A. Woods, N. J. Farrer, M. E. Newton, P. J. Sadler, *J. Am. Chem. Soc.* **2012**, *134*, 16508–16511; b) G. Thiabaud, J. F. Arambula, Z. H. Siddik, J. L. Sessler, *Chem. Eur. J.* **2014**, *20*, 8942–8947; c) J. Kasparkova, H. Kostrhunova, O. Novakova, R. Křikavová, J. Vančo, Z. Trávníček, V. Brabec, *Angew. Chem. Int. Ed.* **2015**, *54*, 14478–14482; *Angew. Chem.* **2015**, *127*, 14686–14690; d) S. Alonso-de Castro, A. L. Cortajarena, F. López-Gallego, L. Salassa, *Angew. Chem. Int. Ed.* **2018**, *57*, 3143–3147; *Angew. Chem.* **2018**, *130*, 3197–3201; e) Z. Wang, N. Wang, S.-C. Cheng, K. Xu, Z. Deng, S. Chen, Z. Xu, K. Xie, M.-K. Tse, P. Shi, H. Hirao, C.-C. Ko, G. Zhu, *Chem* **2019**, *5*, 3151–3165; f) D. J. Norman, A. Gambardella, A. R. Mount, A. F. Murray, M. Bradley, *Angew. Chem. Int. Ed.* **2019**, *58*, 14189–14192; *Angew. Chem.* **2019**, *131*, 14327–14330; g) Z. Deng, C. Li, S. Chen, Q. Zhou, Z. Xu, Z. Wang, H. Yao, H. Hirao, G. Zhu, *Chem. Sci.* **2021**, *12*, 6536–6542; h) Z. Huang, A. P. King, J. Lovett, B. Lai, J. J. Woods, H. H. Harris, J. J. Wilson, *Chem. Commun.* **2021**, *57*, 11189–11192.

[5] a) S. H. C. Askes, A. Bahreman, S. Bonnet, *Angew. Chem. Int. Ed.* **2014**, *53*, 1029–1033; *Angew. Chem.* **2014**, *126*, 1047–1051; b) N. A. Smith, P. Zhang, S. E. Greenough, M. D. Horbury, G. J. Clarkson, D. McFeely, A. Habtemariam, L. Salassa, V. G. Stavros, C. G. Dowson, P. J. Sadler, *Chem. Sci.* **2017**, *8*, 395–404; c) L. N. Lameijer, D. Ernst, S. L. Hopkins, M. S. Meijer, S. H. C. Askes, S. E. Le Dévédec, S. Bonnet, *Angew. Chem. Int. Ed.* **2017**, *56*, 11549–11553; *Angew. Chem.* **2017**, *129*, 11707–11711; d) K. Arora, M. Herroon, M. H. Al-Afyouni, N. P. Toupin, T. N. Rohrabaugh, L. M. Loftus, I. Podgorski, C. Turro, J. J. Kodanko, *J. Am. Chem. Soc.* **2018**, *140*, 14367–14380; e) V. H. S. van Rixel, V. Ramu, A. B. Auyeung, N. Beztsinna, D. Y. Leger, L. N. Lameijer, S. T. Hilt, S. E. Le Dévédec, T. Yildiz, T. Betancourt, M. B. Gildner, T. W. Hudnall, V. Sol, B. Liagre, A. Kornienko, S. Bonnet, *J. Am. Chem. Soc.* **2019**, *141*, 18444–18454; f) N. Toupin, S. J. Steinke, S. Nadella, A. Li, T. N. Rohrabaugh, E. R. Samuels, C. Turro, I. F. Sevrioukova, J. J. Kodanko, *J. Am. Chem. Soc.* **2021**, *143*, 9191–9205.

[6] a) Z. Deng, N. Wang, Y. Liu, Z. Xu, Z. Wang, T.-C. Lau, G. Zhu, *J. Am. Chem. Soc.* **2020**, *142*, 7803–7812; b) F. Barragán, P. Lopez-Senin, L. Salassa, S. Betanzos-Lara, A. Habtemariam, V. Moreno, P. J. Sadler, V. Marchan, *J. Am. Chem. Soc.* **2011**, *133*, 14098–14108.

[7] a) Z. Li, A. David, B. A. Albani, J.-P. Pellois, C. Turro, K. R. Dunbar, *J. Am. Chem. Soc.* **2014**, *136*, 17058–17070; b) M. R. Kim, H. Morrison, S. I. Mohammed, *Anti-Cancer Drugs* **2011**, *22*, 896–904; c) A. Kastl, A. Wilbuer, A. L. Merkel, L. Feng, P. Di Fazio, M. Ocker, E. Meggers, *Chem. Commun.* **2012**, *48*, 1863–1865; d) R. J. Holbrook, D. J. Weinberg, M. D. Peterson, E. A. Weiss, T. J. Meade, *J. Am. Chem. Soc.* **2015**, *137*, 3379–3385; e) A. K. Renfrew, N. S. Bryce, T. Hambley, *Chem. Eur. J.* **2015**, *21*, 15224–15234; f) K. Mitra, S. Gautam, P. Kondaiah, A. R. Chakravarty, *Angew. Chem. Int. Ed.* **2015**, *54*, 13989–13993; *Angew. Chem.* **2015**, *127*, 14195–14199; g) H. Luo, B. Cao, A. S. C. Chan, R. W.-Y. Sun, T. Zou, *Angew. Chem. Int. Ed.* **2020**, *59*, 11046–11052; *Angew. Chem.* **2020**, *132*, 11139–11145; h) B. M. Vickerman, C. P. O'Banion, X. Tan, D. S. Lawrence, *ACS Cent. Sci.* **2021**, *7*, 93–103.

[8] a) C. G. Hartinger, P. J. Dyson, *Chem. Soc. Rev.* **2009**, *38*, 391–401; b) C. S. Allardyce, P. J. Dyson, in *Bioorganometallic Chemistry* (Ed.: G. Simonneaux), Springer, Berlin, Heidelberg, **2006**, pp. 177–210; c) G. Gasser, I. Ott, N. Metzler-Nolte, *J. Med. Chem.* **2011**, *54*, 3–25.

[9] a) L. Messori, G. Marcon, in *Metal Ions in Biolgical Systems, Vol. 42: Metal Complexes in Tumor Diagnosis and as Anticancer Agents*, CRC Press, Boca Raton, FL, **2004**, pp. 385–424; b) I. Ott, *Coord. Chem. Rev.* **2009**, *253*, 1670–1681; c) S. Nobili, E. Mini, I. Landini, C. Gabbiani, A. Casini, L. Messori, *Med. Res. Rev.* **2010**, *30*, 550–580; d) S. J. Berners-Price, in *Bioinorg. Med. Chem.*, Wiley-VCH, Weinheim, **2011**, pp. 197–222; e) C. Gabbiani, M. A. Cinellu, L. Maiore, L. Massai, F. Scaletti, L. Messori, *Inorg. Chim. Acta* **2012**, *393*, 115–124; f) N. Cutillas, G. S. Yellol, C. de Haro, C. Vicente, V. Rodríguez, J. Ruiz, *Coord. Chem. Rev.* **2013**, *257*, 2784–2797; g) B. Bertrand, A. Casini, *Dalton Trans.* **2014**, *43*, 4209–4219; h) T. Zou, C. T. Lum, C.-N. Lok, J.-J. Zhang, C.-M. Che, *Chem. Soc. Rev.* **2015**, *44*, 8786–8801; i) C. Nardon, D. Fregona, *Curr. Top. Med. Chem.* **2016**, *16*, 360–380; j) J. Wirmer-Bartoschek, L. E. Bendel, H. R. A. Jonker, J. T. Grün, F. Papi, C. Bazzicalupi, L.

Messori, P. Gratteri, H. Schwalbe, *Angew. Chem. Int. Ed.* **2017**, *56*, 7102–7106; *Angew. Chem.* **2017**, *129*, 7208–7212; k) A. Casini, R. W.-Y. Sun, I. Ott, in *Metallo-Drugs: Development and Action of Anticancer Agents* (Eds.: S. Astrid, S. Helmut, F. Eva, K. O. S. Roland), De Gruyter, Berlin, **2018**, pp. 199–218; l) F. Guarra, A. Terenzi, C. Pirker, R. Passannante, D. Baier, E. Zangrando, V. Gómez-Vallejo, T. Biver, C. Gabbiani, W. Berger, J. Llop, L. Salassa, *Angew. Chem. Int. Ed.* **2020**, *59*, 17130–17136; *Angew. Chem.* **2020**, *132*, 17278–17284; m) S. R. Thomas, A. Casini, *Curr. Opin. Chem. Biol.* **2020**, *55*, 103–110.

[10] a) A. Casini, C. Hartinger, C. Gabbiani, E. Mini, J. Dyson Paul, K. Keppler Bernard, L. Messori, *J. Inorg. Biochem.* **2008**, *102*, 564–575; b) A. Bindoli, M. P. Rigobello, G. Scutari, C. Gabbiani, A. Casini, L. Messori, *Coord. Chem. Rev.* **2009**, *253*, 1692–1707; c) C. Gabbiani, L. Messori, *Anti-Cancer Agents Med. Chem.* **2011**, *11*, 929–939; d) A. Casini, L. Messori, *Curr. Top. Med. Chem.* **2011**, *11*, 2647–2660; e) M. Mora, M. C. Gimeno, R. Visbal, *Chem. Soc. Rev.* **2019**, *48*, 447–462; f) A. Giorgio, A. Merlino, *Coord. Chem. Rev.* **2020**, *407*, 213175; g) T. Gamberi, A. Pratesi, L. Messori, L. Massai, *Coord. Chem. Rev.* **2021**, *438*, 213905.

[11] A. J. Bard, R. Parsons, J. Jordan, in *Standard Potentials in Aqueous Solution*, CRC Press, Boca Raton, FL, **1985**, pp. 287–320.

[12] a) S. J. Berners-Price, C. K. Mirabelli, R. K. Johnson, M. R. Mattern, F. L. McCabe, L. F. Faucette, C.-M. Sung, S.-M. Mong, P. J. Sadler, S. T. Crooke, *Cancer Res.* **1986**, *46*, 5486–5493; b) A. Meyer, C. P. Bagowski, M. Kokoschka, M. Stefanopoulou, H. Alborzinia, S. Can, D. H. Vlecken, W. S. Sheldrick, S. Wölfl, I. Ott, *Angew. Chem. Int. Ed.* **2012**, *51*, 8895–8899; *Angew. Chem.* **2012**, *124*, 9025–9030; c) J. Fernández-Gallardo, B. T. Elie, T. Sadhukha, S. Prabha, M. Sanaú, S. A. Rotenberg, J. W. Ramos, M. Contel, *Chem. Sci.* **2015**, *6*, 5269–5283; d) J.-J. Zhang, M. A. Abu el Maaty, H. Hoffmeister, C. Schmidt, J. K. Muenzner, R. Schobert, S. Wölfl, I. Ott, *Angew. Chem. Int. Ed.* **2020**, *59*, 16795–16800; *Angew. Chem.* **2020**, *132*, 16940–16945.

[13] a) P. J. Barnard, L. E. Wedlock, M. V. Baker, S. J. Berners-Price, D. A. Joyce, B. W. Skelton, J. H. Steer, *Angew. Chem. Int. Ed.* **2006**, *45*, 5966–5970; *Angew. Chem.* **2006**, *118*, 6112–6116; b) J. L. Hickey, R. A. Ruhayel, P. J. Barnard, M. V. Baker, S. J. Berners-Price, A. Filipovska, *J. Am. Chem. Soc.* **2008**, *130*, 12570–12571; c) T. Zou, C. T. Lum, S. S.-Y. Chui, C.-M. Che, *Angew. Chem. Int. Ed.* **2013**, *52*, 2930–2933; *Angew. Chem.* **2013**, *125*, 3002–3005; d) T. Zou, C. T. Lum, C.-N. Lok, W.-P. To, K.-H. Low, C.-M. Che, *Angew. Chem. Int. Ed.* **2014**, *53*, 5810–5814; *Angew. Chem.* **2014**, *126*, 5920–5924; e) C. Bazzicalupi, M. Ferraroni, F. Papi, L. Massai, B. Bertrand, L. Messori, P. Gratteri, A. Casini, *Angew. Chem. Int. Ed.* **2016**, *55*, 4256–4259; *Angew. Chem.* **2016**, *128*, 4328–4331; f) C. Zhang, P.-Y. Fortin, G. Barnoin, X. Qin, X. Wang, A. Fernandez Alvarez, C. Bijani, M.-L. Maddelein, C. Hemmert, O. Cuvillier, H. Gornitzka, *Angew. Chem. Int. Ed.* **2020**, *59*, 12062–12068; *Angew. Chem.* **2020**, *132*, 12160–12166.

[14] a) Z. Yang, G. Jiang, Z. Xu, S. Zhao, W. Liu, *Coord. Chem. Rev.* **2020**, *423*, 213492; b) V. Fernández-Moreira, I. Marzo, M. C. Gimeno, *Chem. Sci.* **2014**, *5*, 4434–4446.

[15] C. Marzano, L. Ronconi, F. Chiara, M. C. Giron, I. Faustinelli, P. Cristofori, A. Trevisan, D. Fregona, *Int. J. Cancer* **2011**, *129*, 487–496.

[16] D. Hu, Y. Liu, Y.-T. Lai, K.-C. Tong, Y.-M. Fung, C.-N. Lok, C.-M. Che, *Angew. Chem. Int. Ed.* **2016**, *55*, 1387–1391; *Angew. Chem.* **2016**, *128*, 1409–1413.

[17] a) L. Messori, G. Marcon, M. A. Cinellu, M. Coronnello, E. Mini, C. Gabbiani, P. Orioli, *Bioorg. Med. Chem.* **2004**, *12*, 6039–6043; b) M. Frik, J. Fernández-Gallardo, O. Gonzalo, V. Mangas-Sanjuan, M. González-Alvarez, A. Serrano del Valle, C. Hu, I. González-Alvarez, M. Bermejo, I. Marzo, M. Contel, *J. Med. Chem.* **2015**, *58*, 5825–5841; c) S. K. Fung, T. Zou, B. Cao, P. Y. Lee, Y. M. E. Fung, D. Hu, C.-N. Lok, C.-M. Che, *Angew. Chem. Int. Ed.* **2017**, *56*, 3892–3896; *Angew. Chem.* **2017**, *129*, 3950–3954.

[18] a) D. K. Crites Tears, D. R. McMillin, *Coord. Chem. Rev.* **2001**, *211*, 195–205; b) J. L. Retsek, C. M. Drain, C. Kirmaier, D. J. Nurco, C. J. Medforth, K. M. Smith, I. V. Sazanovich, V. S. Chirvony, J. Fajer, D. Holten, *J. Am. Chem. Soc.* **2003**, *125*, 9787–9800.

[19] a) D. B. Pourreau, G. L. Geoffroy, in *Adv. Organomet. Chem., Vol. 24* (Eds.: F. G. A. Stone, R. West), Academic Press, San Diego, **1985**, pp. 249–352; b) A. T. Hutton, in *Inorganic Reactions and Methods*, Wiley, New York, **1991**, pp. 26–32; c) C. Elschenbroich, in *Organometallics*, Wiley-VCH, Weinheim, **2006**, pp. 291–315.

[20] a) E. A. Glascoe, M. F. Kling, J. E. Shanoski, R. A. DiStasio, C. K. Payne, B. V. Mork, T. D. Tilley, C. B. Harris, *Organometallics* **2007**, *26*, 1424–1432; b) F. Rekhroukh, L. Estevez, S. Mallet-Ladeira, K. Miqueu, A. Amgoune, D. Bourissou, *J. Am. Chem. Soc.* **2016**, *138*, 11920–11929; c) R. Kumar, J.-P. Krieger, E. Gómez-Bengoa, T. Fox, A. Linden, C. Nevado, *Angew. Chem. Int. Ed.* **2017**, *56*, 12862–12865; *Angew. Chem.* **2017**, *129*, 13042–13045; d) R. P. Herrera, M. C. Gimeno, *Chem. Rev.* **2021**, *121*, 8311–8363.

[21] W.-P. To, G. S. M. Tong, C.-W. Cheung, C. Yang, D. Zhou, C.-M. Che, *Inorg. Chem.* **2017**, *56*, 5046–5059.

[22] A. Bahreman, J.-A. Cuello-Garibo, S. Bonnet, *Dalton Trans.* **2014**, *43*, 4494–4505.

[23] G. R. Fulmer, A. J. M. Miller, N. H. Sherden, H. E. Gottlieb, A. Nudelman, B. M. Stoltz, J. E. Bercaw, K. I. Goldberg, *Organometallics* **2010**, *29*, 2176–2179.

[24] J. Diaz, K. Rich, S. Munie, C. R. Zoch, J. L. Hubbard, A. S. Larsen, *Polyhedron* **2016**, *114*, 435–442.

[25] A. L. Ortega, S. Mena, J. M. Estrela, *Cancers* **2011**, *3*, 1285–1310.

[26] a) C. Bronner, O. S. Wenger, *Dalton Trans.* **2011**, *40*, 12409–12420; b) M.-C. Tang, M.-Y. Chan, V. W.-W. Yam, *Chem. Rev.* **2021**, *121*, 7249–7279.

[27] S.-W. Lai, C.-M. Che, *Top. Curr. Chem.* **2004**, *241*, 27–63.

[28] C. J. Ballhausen, N. Bjerrum, R. Dingle, K. Eriks, C. R. Hare, *Inorg. Chem.* **1965**, *4*, 514–518.

[29] Ö. Karaca, V. Scalcon, S. M. Meier-Menches, R. Bonsignore, J. M. J. L. Brouwer, F. Tonolo, A. Folda, M. P. Rigobello, F. E. Kühn, A. Casini, *Inorg. Chem.* **2017**, *56*, 14237–14250.

[30] L. Massai, C. Zoppi, D. Cirri, A. Pratesi, L. Messori, *Front. Chem.* **2020**, *8*, 581648.

[31] a) S. Chen, R. Costil, F. K.-C. Leung, B. L. Feringa, *Angew. Chem. Int. Ed.* **2021**, *60*, 11604–11627; *Angew. Chem.* **2021**, *133*, 11708–11731; b) K.-C. Tong, P.-K. Wan, C.-N. Lok, C.-M. Che, *Chem. Sci.* **2021**, *12*, 15229–15238.

[32] a) M. Patra, T. C. Johnstone, K. Suntharalingam, S. J. Lippard, *Angew. Chem. Int. Ed.* **2016**, *55*, 2550–2554; *Angew. Chem.* **2016**, *128*, 2596–2600; b) L. N. Lameijer, S. L. Hopkins, T. G. Brevé, S. H. C. Askes, S. Bonnet, *Chem. Eur. J.* **2016**, *22*, 18484–18491; c) A. Pettenuzzo, K. Vezzù, M. L. Di Paolo, E. Fotopoulou, L. Marchiò, L. D. Via, L. Ronconi, *Dalton Trans.* **2021**, *50*, 8963–8979.

[33] S. Alonso-de Castro, E. Ruggiero, A. Ruiz-de-Angulo, E. Rezabal, J. C. Mareque-Rivas, X. Lopez, F. López-Gallego, L. Salassa, *Chem. Sci.* **2017**, *8*, 4619–4625.

Manuscript received: January 20, 2022
Accepted manuscript online: February 14, 2022
Version of record online: February 21, 2022